J|A|C|S
ARTICLES
Published on Web 08/27/2003

Infrared Spectra and Structures of the Stable CuH_2^-, AgH_2^-, AuH_2^-, and AuH_4^- Anions and the AuH_2 Molecule

Lester Andrews* and Xuefeng Wang

Contribution from the Department of Chemistry, University of Virginia, McCormick Road, P.O. Box 400319, Charlottesville, Virginia 22904-4319

Received May 23, 2003; E-mail: lsa@virginia.edu

Abstract: Gold is noble, but excited gold is reactive. Reactions of laser-ablated copper, silver, and gold with H_2 in excess argon, neon, and pure hydrogen during condensation at 3.5 K give the MH molecules and the $(H_2)MH$ complexes as major products and the MH_2^- and AuH_4^- anions as minor products. These new molecular anions are identified from matrix infrared spectra with isotopic substitution (HD, D_2, and $H_2 + D_2$) and comparison to frequencies calculated by density functional theory. The stable linear MH_2^- anions are unique in that their corresponding neutral MH_2 molecules are higher in energy than $M + H_2$ and thus unstable to $M + H_2$ decomposition. Infrared spectra are observed for the bending modes of AuH_2, AuHD, and AuD_2 in solid H_2, HD, and D_2, respectively. The observation of square-planar AuH_4^- attests the stability of the higher Au(III) oxidation state for gold. The synthesis of CuH_2^- in solid compounds has potential for use in hydrogen storage.

Introduction

Gold is the least reactive of the coinage metals, but gold reacts readily with halogens. The chemistry of copper(I), silver(I), and gold(I) halide complexes is well-known.[1] The solubility of the group 11 metal chlorides increases in HCl solution due to the formation of stable MCl_2^- complexes. The $CuCl_2^-$ and $CuBr_2^-$ anions have been characterized recently by PES in the gas phase and by electronic structure calculations.[2] The stable $AgCl_2^-$ anion has been prepared, and the linear structure determined by X-ray diffraction.[3] A very recent investigation of gas phase $AuCl_2^-$ and $AuBr_2^-$ has determined electron detachment energies and predicted stable neutral dihalide molecules.[4] In addition, Au(III) compounds are stable, and Au(I) complexes disproportionate to Au(III) compounds and gold in aqueous solutions.[1] Accordingly, the $AuCl_2^-$ and $AuBr_2^-$ anions can be photooxidized to $AuCl_4^-$ and $AuBr_4^-$ in the presence of electron acceptors.[5] Finally, the trend in observed force constants k(Au−L) > k(Cu−L) > k(Ag−L) (L = Cl^-, Br^-, I^-) and the stability of Au(III) compounds have been explained by relativistic effects.[6,7]

Metal hydrides are important as a source of hydrogen for portable fuel cells.[8] For example, the Mg_2NiH_4 compound is a promising hydrogen storage material.[9] Understanding the stability of metal hydrides is central to the design of new materials for hydrogen storage.[10] In addition nickel/metal hydride batteries are used in many commercial applications.[11] In the course of a matrix-isolation investigation of copper, silver, and gold (group 11) hydrides, we discovered the MH_2^- anions, which have unique properties. Our density functional theory (DFT) calculations show that these MH_2^- anions are very stable, but the corresponding neutral MH_2 molecules, which have also been computed by others,[6,12−15] are higher in energy than M and H_2. Four late first-row transition metal dihydride anions (MnH_2^- through NiH_2^-) have been characterized by photoelectron spectroscopy (PES),[16] but the neutral molecules are stable in contrast to CuH_2.[17−21] Although there are many examples of homoleptic transition metal hydride anions, the only known group 11 hydride anion is CuH_4^{3-} in solid Ba/Cu alloys under H_2 pressure.[22,23]

(1) Cotton, F. A.; Wilkinson, G.; Murillo, C. A.; Bochmann, M. *Advanced Inorganic Chemistry*, 6th ed.; Wiley: New York, 1999.
(2) Wang, X.-B.; Wang, L.-S.; Brown, R.; Schwerdtfeger, P.; Schröder, D.; Schwarz, H. *J. Chem. Phys.* **2001**, *114*, 7388.
(3) Helgesson, G.; Jagner, S. *Inorg. Chem.* **1991**, *30*, 2574.
(4) Schröder, D.; Brown, R.; Schwerdtfeger, P.; Wang, X. B.; Yang, X.; Wang, L. S.; Schwarz, H. *Angew. Chem., Int. Ed.* **2003**, *42*, 311.
(5) Kunkely, H.; Vogler, A. *Inorg. Chem.* **1992**, *31*, 4539.
(6) Schwerdtfeger, P.; Boyd, P. D. W.; Burrell, A. K.; Robinson, W. T.; Taylor, M. J. *Inorg. Chem.* **1990**, *29*, 3593.
(7) Schwerdtfeger, P.; Boyd, P. D. W.; Brienne, S.; Burrell, A. K. *Inorg. Chem.* **1992**, *31*, 3411, and references therein.
(8) Schlapbach, Z. A. *Nature* (*London*) **2001**, *414*, 353.
(9) Häussermann, U.; Blomqvist, H.; Noréus, D. *Inorg. Chem.* **2002**, *41*, 3684.
(10) Smithson, H.; Marianetti, C. A.; Morgan, D.; Van der Ven, A.; Predith, A.; Ceder, G. *Phys. Rev. B* **2002**, *66*, 144107.
(11) Sandrock, G.; Thomas, G. In *Hydride Information Center*, http://hydpark.ca.sandia.gov/; Sandia National Laboratories: Livermore, CA, 2001.
(12) Siegbahn, P. E. M.; Blomberg, M. R. A.; Bauschlicher, C. W. *J. Chem. Phys.* **1984**, *81*, 1373.
(13) Niu, J.; Rao, B. K.; Jena, B. *Phys. Rev. B* **1995**, *51*, 4475.
(14) Garcia-Prieto, J.; Ruiz, M. E.; Novaro, O. *J. Am. Chem. Soc.* **1985**, *107*, 5635.
(15) (a) Balusubramanian, K.; Liao, M. J. *J. Phys. Chem.* **1988**, *92*, 361. (b) Balusubramanian, K.; Liao, M. J. *J. Phys. Chem.* **1989**, *93*, 89. (c) Balasubramanian, K. *J. Phys. Chem.* **1989**, *93*, 6585.
(16) Miller, A. E. S.; Feigerle, C. S.; Lineberger, W. C. *J. Chem. Phys.* **1986**, *84*, 4127.
(17) Wang, X.; Andrews, L. *J. Phys. Chem. A* **2003**, *107*, 4081 (MnH_2).
(18) Chertihin, G. V.; Andrews, L. *J. Phys. Chem.* **1995**, *99*, 1214.
(19) Billups, W. E.; Chang, S.-C.; Hauge, R. H.; Margrave, J. L. *J. Am. Chem. Soc.* **1995**, *117*, 1387.
(20) Li, S.; Van Zee, R. J.; Weltner, W., Jr.; Cory, M. G.; Zerner, M. C. *J. Chem. Phys.* **1997**, *106*, 2055.
(21) (a) Ozin, G. A.; Mitchell, S. A.; Garcia Prieto, J. *Angew. Chem., Int. Ed. Engl.* **1982**, *21*, 380. (b) Ozin, G. A.; Gracie, C. *J. Phys. Chem.* **1984**, *88*, 643.

Despite the extensive chemistry for group 11 metal dihalide complexes, the corresponding metal dihydrides are unknown. The coinage metal diatomic metal hydride molecules have been characterized in the gas phase by emission spectroscopy.[24] An important theoretical study, however, predicted that AuH will add H^- to form AuH_2^-.[6] This is mechanistically significant, as the neutral MH_2 dihydrides are unstable relative to $M + H_2$, in contrast to the corresponding MX_2 dihalides.[2,4] Calculations have been performed for CuH_2, AgH_2, and AuH_2, and these bent $^2B_2$ ground state molecules range from 6 to 43 to 20 kcal/mol, respectively, higher in energy than $M + H_2$.[14,15] Hence, preparation of the MH_2^- anions will be experimentally difficult, as formation of the MH_2 molecules requires excited metal atom reactions. Although ground state copper (^2S) does not react with H_2, excited Cu (^2P) reacts spontaneously to form CuH + H in solid krypton.[21] However, the back reaction that might synthesize CuH_2 on annealing the sample instead restores the lower energy $Cu + H_2$ reagents. Hence, CuH_2 is unstable and dissociation back to Cu and H_2 is favored. Since the AuH bond is stronger than the CuH bond,[24] the AuH_2 molecule has a better chance of survival.

Our investigation of group 11 hydrides involves the reaction of energetic laser-ablated metal atoms[25] and H_2 in excess argon, neon, and hydrogen. All of the group 11 metal hydrides, MH, and dihydrogen complexes, $(H_2)MH$, have been observed by matrix infrared spectroscopy and confirmed by comparison to DFT calculated frequencies.[26] We describe here the formation of the stable linear coinage metal MH_2^- anions and the related square-planar AuH_4^- anion, and DFT calculations of their structures and vibrational frequencies.

Experimental and Theoretical Methods

Laser-ablated copper, silver, and gold atoms were reacted with H_2, D_2, and HD in excess argon and neon, and with pure H_2, HD, and D_2 during condensation at 3.5 K using methods described previously for gold carbonyls[27,28] and for vanadium and chromium hydrides using pure hydrogen as a reactive matrix host.[29,30] Infrared (IR) spectra were recorded at 0.5 or 1.0 cm^{-1} resolution using an HgCdTeB detector on a Nicolet 750 FTIR, samples were annealed and irradiated by ultraviolet and visible light (Philips, 175 W), and more spectra were recorded.

Complementary density functional theory DFT calculations were performed using the Gaussian 98 program,[31] the BPW91 and B3LYP density functionals,[32,33] the 6-311++G(d,p) basis for H, and SDD effective core potential and basis sets for the metals as given in Gaussian 98.[34,35] Relativistic effects were included by adjusting the pseudopotential parameters to spin−orbit averaged Dirac−Fock energies.[35] Vibrational frequencies were computed analytically from the potential energy surface in the harmonic approximation at the optimized structures: the calculated frequencies reported here are not scaled. The BPW91 functional has been recommended for group 11 metal-containing molecules after comparison of results using several methods, although the B3LYP functional works almost as well.[36] The BPW91 and B3LYP functionals gave frequencies within 1% and bond lengths within 0.01 Å.

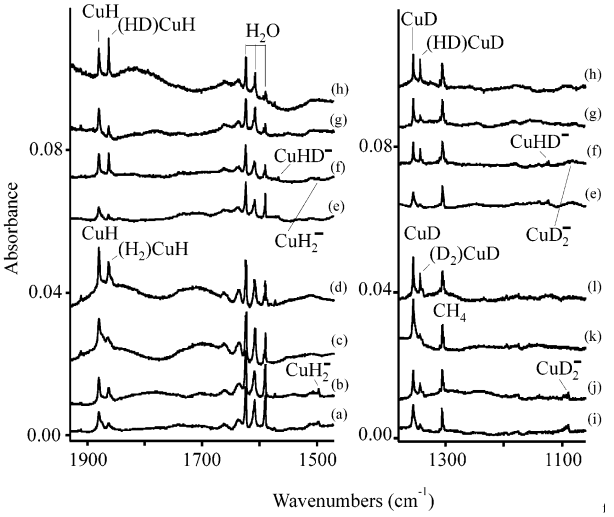

Figure 1. Infrared spectra of copper hydrides in the Cu−H and Cu−D stretching regions: (a) 5% H_2 in argon co-deposited with laser-ablated Cu at 3.5 K for 60 min, (b) after annealing to 15 K, (c) after $\lambda > 240$ nm photolysis for 15 min, (d) after annealing to 20 K, (e) 5% HD in argon co-deposited with laser-ablated Cu at 3.5 K for 60 min, (f) after annealing to 19 K, (g) after $\lambda > 240$ nm photolysis for 15 min, (h) after annealing to 25 K, (i) 5% D_2 in argon co-deposited with laser-ablated Cu at 3.5 K for 60 min, (j) after annealing to 15 K, (k) after $\lambda > 240$ nm photolysis for 15 min, and (l) after annealing to 20 K.

Results and Discussion

CuH_2^- and CuD_2^-. IR spectra in the Cu−H and Cu−D stretching regions are shown in Figure 1 for laser-ablated Cu reaction products with H_2 and D_2 in excess argon, and the observed frequencies are listed in Table 1. Weak bands are observed at 1879.8, 1862.5, and 1497.2 cm^{-1} in the Cu−H region and at 1354.9, 1343.2, and 1089.4 cm^{-1} in the Cu−D region. Annealing to 15 K slightly increases all of these absorptions, but $\lambda > 240$ nm photolysis increases the first, decreases the second, and destroys the third band in each region. A subsequent annealing to 20 K sharpens the first, increases the second, and has no regenerative effect on the third band. The HD reagent reveals important diagnostic information: the 1879.8 and 1354.9 cm^{-1} bands are unchanged, the 1862.5 and 1343.2 cm^{-1} bands are each shifted 0.2 cm^{-1}, and the 1497.2 and 1089.4 cm^{-1} absorptions are observed along with new, stronger 1566.9 and 1122.7 cm^{-1} bands. With $H_2 + D_2$ the 1879.8 and 1354.9 cm^{-1} bands were also unchanged, but the

(22) Huang, B.; Fauth, F.; Yvon, K. *J. Alloys Compd.* **1996**, *L1*, 244.
(23) King, R. B. *Coord. Chem. Rev.* **2000**, *200−202*, 813.
(24) Huber, K. P.; Herzberg, G. *Molecular Spectra and Molecular Structure, Vol. IV, Constants of Diatomic Molecules*; Van Nostrand Reinhold: New York, 1979.
(25) Kang, H.; Beauchamp, J. L. *J. Phys. Chem.* **1985**, *89*, 3364.
(26) Wang, X.; Andrews, L.; Manceron, L.; Marsden, C. *J. Phys. Chem. A* **2003**, *107*, in press.
(27) Liang, B.; Andrews, L. *J. Phys. Chem. A* **2000**, *104*, 9156.
(28) Andrews, L.; Citra, A. *Chem. Rev.* **2002**, *102*, 885.
(29) Weltner, W., Jr.; Van Zee, R. J.; Li, S. *J. Phys. Chem.* **1995**, *99*, 6277.
(30) Wang, X.; Andrews, L. *J. Phys. Chem. A* **2003**, *107*, 570 (Cr + H_2).
(31) Frisch, M. J.; Trucks, G. W.; Schlegel, H. B.; Scuseria, G. E.; Robb, M. A.; Cheeseman, J. R.; Zakrzewski, V. G.; Montgomery, J. A., Jr.; Stratmann, R. E.; Burant, J. C.; Dapprich, S.; Millam, J. M.; Daniels, A. D.; Kudin, K. N.; Strain, M. C.; Farkas, O.; Tomasi, J.; Barone, V.; Cossi, M.; Cammi, R.; Mennucci, B.; Pomelli, C.; Adamo, C.; Clifford, S.; Ochterski, J.; Petersson, G. A.; Ayala, P. Y.; Cui, Q.; Morokuma, K.; Malick, D. K.; Rabuck, A. D.; Raghavachari, K.; Foresman, J. B.; Cioslowski, J.; Ortiz, J. V.; Stefanov, B. B.; Liu, G.; Liashenko, A.; Piskorz, P.; Komaromi, I.; Gomperts, R.; Martin, R. L.; Fox, D. J.; Keith, T.; Al-Laham, M. A.; Peng, C. Y.; Nanayakkara, A.; Gonzalez, C.; Challacombe, M.; Gill, P. M. W.; Johnson, B.; Chen, W.; Wong, M. W.; Andres, J. L.; Gonzalez, C.; Head-Gordon, M.; Replogle, E. S.; Pople, J. A. *Gaussian 98*, Revision A.6; Gaussian, Inc.: Pittsburgh, PA, 1998.
(32) (a) Becke, A. D. *Phys. Rev. A* **1988**, *38*, 3098. (b) Perdew, J. P.; Wang, Y. *Phys. Rev. B* **1992**, *45*, 13244.
(33) (a) Becke, A. D. *J. Chem. Phys.* **1993**, *98*, 5648. (b) Lee, C.; Yang, W.; Parr, R. G. *Phys. Rev. B* **1988**, *37*, 785.
(34) (a) Krishnan, R.; Binkley, J. S.; Seeger, R.; Pople, J. A. *J. Chem. Phys.* **1980**, *72*, 650. (b) Frisch, M. J.; Pople, J. A.; Binkley, J. S. *J. Chem. Phys.* **1984**, *80*, 3265.
(35) Schwerdtfeger, P.; Schwarz, W. H. E.; Bowmaker, G. A.; Boyd, P. D. W. *J. Chem. Phys.* **1989**, *91*, 1762.
(36) Legge, F. S.; Nyberg, G. L.; Peel, J. B. *J. Phys. Chem. A* **2001**, *105*, 7905.

Table 1. Infrared Absorptions (cm^{-1}) Observed from Copper, Silver, and Gold Atom Reactions with Dihydrogen in Excess Argon, Neon, and Hydrogen

argon			neon			hydrogen			
H_2	HD	D_2	H_2	HD	D_2	H_2	HD	D_2	identification
1879.8	1879.8		1889.9	1889.9					CuH
	1354.9	1354.9		1362.2	1362.2				CuD
1862.5	1862.7		1869.1	1869.1		1861.4	1865.5		$(H_2)CuH$
	1343.0	1343.2		1346.4	1344.9		1345.4	1341.6	$(D_2)CuD$
1497.2	1566.9		1529.5			1517.8	1586.7		CuH_2^-
	1122.7	1089.4		1158.3	1116.5		1137.6	1107.3	CuD_2^-
1717.0	1717.0								AgH
	1233.8	1233.8							AgD
1746.5	1748.2		1750.8			1742.6	1748.6		$(H_2)AgH$
	1256.9	1257.6			1264.3		1255.4	1255.7	$(D_2)AgD$
1427.5	1496.8		1460			1442.4			AgH_2^-
	1068.9	1032.3			1053			1045.9	AgD_2^-
2226.6									AuH
		1597.2							AuD
2173.6, 2170.6			2170.1, 2167.9			2164.0			$(H_2)AuH$
		1559.3			1559.0			1556.5	$(D_2)AuD$
						1676.4	1840.4		AuH_4^-
1642			1684	1831		1661.5	1821		$(H_2)AuH_3$
			1638.6			1636.0			AuH_2^-
							1280.4	1212.2	AuD_4^-
		1182		1275	1207		1257	1198.6	$(D_2)AuD_3$
								1182.3	AuD_2^-
						638.1			AuH_2
							570.6		AuHD
								457.0	AuD_2

1497.2 and 1089.4 cm^{-1} absorptions were stronger than the 1566.9 and 1122.7 cm^{-1} bands.

The 1879.8 and 1354.9 cm^{-1} bands, which were unshifted with HD, are due to CuH and CuD in solid argon.[26] These bands are blue shifted 13.5 and 8.2 cm^{-1} from the gas phase[24] values owing to matrix repulsion as observed for AuH and AuD.[37,38] Our BPW91 calculation predicts these harmonic frequencies at 1947.1 and 1388.1 cm^{-1} (Table 2) with a CuH/CuD ratio of 1.403. The observed frequencies are slightly lower and exhibit a lower CuH/CuD ratio of 1.387 because of anharmonicity. The slightly shifted 1862.5 and 1343.2 cm^{-1} bands exhibit the same 1.387 H/D ratio as CuH/CuD and are assigned to the $(H_2)CuH$ and $(D_2)CuD$ complexes. In pure solid H_2 and D_2, the CuH and CuD molecules are not observed, but the $(H_2)CuH$ and (D_2)-CuD complex bands are stronger at 1861.4 and 1341.6 cm^{-1} with weaker associated H−H and D−D stretching modes at 3566.6 and 2582.0 cm^{-1}. Infrared spectra for Cu in pure H_2 and pure HD are compared in Figure 2.

The photosensitive 1497.2 and 1089.4 cm^{-1} bands in solid argon are observed at 1517.8 and 1107.3 cm^{-1} in solid H_2 and D_2 and at 1529.5 and 1116.5 cm^{-1} in excess neon (Table 1). The 1517.8 cm^{-1} band decreased 50% on $\lambda > 470$ nm photolysis and disappeared with $\lambda > 240$ nm irradiation. These band pairs exhibit 1.372 ± 0.002 H/D ratios and are too low for a neutral copper hydride. In pure HD the spectrum gives a new 1586.7 cm^{-1} absorption and no 1517.8 cm^{-1} band in the Cu−H region and a new 1137.6 cm^{-1} absorption and no 1107.3 cm^{-1} band in the Cu−D region (not shown). The CuH_2 molecule stretching frequencies are computed in the 1600−1800 cm^{-1} region (Tables 2, 3), and since CuH_2 is higher in energy than Cu + H_2, it is not expected to survive in significant yield.[14] Although photochemical experiments with Cu and H_2 in solid krypton formed CuH and not CuH_2,[21] hydrogen matrix experiments provide evidence for CuH_2.[26]

Therefore, the simple CuH_2^- anion, which is expected to be stable like the isoelectronic closed-shell ZnH_2 molecule,[39] must be considered. The very intense antisymmetric stretching (σ_u) modes calculated at 1501.0 cm^{-1} for the linear CuH_2^- anion and at 1078.1 cm^{-1} for the CuD_2^- isotopomer (ratio 1.392) (Table 2) are in excellent agreement with the present observations. The observed H/D ratio 1.374 is less than the calculated 1.392 ratio owing to anharmonicity. Both of these ratios are less than the CuH/CuD ratio for the diatomic molecule because the antisymmetric stretching mode of a linear H−Cu−H subunit has more Cu and less H participation than the Cu−H diatomic vibration. Furthermore the unobserved symmetric stretching (σ_g) mode is higher than the σ_u mode, and the $HCuD^-$ anion is calculated to have Cu−H and Cu−D stretching absorptions at 1600.7 and 1121.9 cm^{-1}, which are 6.6 and 4.1% higher than the σ_u modes calculated for CuH_2^- and CuD_2^-. The observed $HCuD^-$ bands are 4.7 and 3.1% higher (argon matrix). This agreement between calculated and observed frequencies for CuH_2^-, $CuHD^-$, and CuD_2^- confirms our identification of CuH_2^-. The CuH_2^- anion is 57 kcal/mol more stable than CuH_2 at the B3LYP level of theory. We have no evidence for metal hydride cation species: the stable $Cu(H_2)^+$ complex absorptions (Table 2) are not detected. The Ar_nH^+ and Ar_nD^+ cations provide for charge balance in the argon matrix.[40,41]

AgH_2^- and AgD_2^-. Analogous bands for AgH and (H_2)-AgH (Table 1) were observed with laser-ablated silver.[26] In addition new photosensitive bands were found at 1460 and 1053 cm^{-1} in excess neon, at 1442.4 and 1045.9 cm^{-1} in pure solid H_2 and solid D_2 (Figure 3), and at 1427.5 and 1032.3 cm^{-1} in excess argon. Photolysis with wavelengths > 380 and 290 nm slightly increased the 1442.4 cm^{-1} band, and 240 nm photolysis almost destroyed it. These band pairs exhibit 1.383 ± 0.004

(37) Wang, X.; Andrews, L. *J. Am. Chem. Soc.* **2001**, *123*, 12899.
(38) Wang, X.; Andrews, L. *J. Phys. Chem. A* **2002**, *106*, 3744 (Au + H_2).
(39) Greene, T. M.; Brown, W.; Andrews, L.; Downs, A. J.; Chertihin, G. V.; Runeberg, N.; Pyykkö, P. *J. Phys. Chem.* **1995**, *99*, 7925.
(40) Milligan, D. E.; Jacox, M. E. *J. Mol. Spectrosc.* **1973**, *46*, 460.
(41) Wight, C. A.; Ault, B. S.; Andrews, L. *J. Chem. Phys.* **1976**, *65*, 1244.

Table 2. States, Structures, and Vibrational Frequencies (cm^{-1}) Calculated for Copper, Silver, and Gold Hydrides Using BPW91/6-311++G(d,p)/SDD

species	state	Å, deg	frequencies, cm^{-1} (mode symmetry, intensity, km/mol)
CuH	$^1\Sigma^+$	1.456	CuH: 1947(26); CuD: 1388(13)
CuH_2	$^2B_2$	1.515 124.1	CuH_2: 1770(a_1,6), 1631(b_2,5), 637(a_1,75)
CuH_2^-[a] ($D_{\infty h}$)	$^1\Sigma_g^+$	1.560	CuH_2^-: 1687(σ_g, 0), 1501(σ_u, 838), 643(π_u, 177 × 2) $CuHD^-$: 1601(330), 1122(295), 560(130 × 2) CuD_2^-: 1187(0), 1078(413), 462(83 × 2)
CuH_4^- (D_{4h})	$^1A_{1g}$	1.527	1804(b_{1g}, 0), 1766(a_{1g}, 0), 1605(e_u, 988 × 2), 759(σ_u, 931), 722(a_{2u}, 34), 688(a_{2u}, 175), 521(e_u, 66 × 2)
AgH	$^1\Sigma^+$	1.608	AgH: 1804(43); AgD: 1282(22)
AgH_2	$^2B_2$	1.655 120.3°	AgH_2: 1683(a_1,5), 1541(b_2,1), 537(a_1,74)
AgH_2^-[a] ($D_{\infty h}$)	$^1\Sigma_g^+$	1.699	AgH_2^-: 1619(σ_g, 0), 1445(σ_u, 931), 620(π_u, 167 × 2) $AgHD^-$: 1543(363), 1077(334), 539(124 × 2) AgD_2^-: 1145(0), 1031(462), 442(80 × 2)
AgH_4^- (D_{4h})	$^1A_{1g}$	1.656	1815(b_{1g}, 0), 1805(a_{1g}, 0), 1604(e_u, 1018 × 2), 745(b_{2u}, 0), 692(a_{2u}, 34, 118), 681(e_u, 27 × 2), 633(e_u, 49 × 2)
AuH	$^1\Sigma^+$	1.546	AuH: 2227 (15); AuD: 1580 (8)
AuH_2	$^2B_2$	1.619 129.1	AuH_2: 2004(a_1, 1), 1758(b_1, 0.5), 666(a_1, 25) AuHD: 1900 (1), 1315(0.4), 579 (19) AuD_2: 1419 (1), 1249 (0.2), 473 (12)
AuH_2^-[a] ($D_{\infty h}$)	$^1\Sigma_g^+$	1.668	AuH_2^-: 1946(σ_u, 0), 1642(σ_u, 1068), 731(π_u, 41 × 2) $AuHD^-$: 1824(360), 1242(440), 634(30 × 2) AuD_2^-: 1377(0), 1167(532), 520(19 × 2)
AuH_4^- (D_{4h})	$^1A_{1g}$	1.653	AuH_4^-: 2030(b_{1g}, 0), 2029(a_{1g}, 0), 1724(e_u, 1082 × 2), 799(b_{2u}, 0), 789(a_{2u}, 34), 762(e_u, 27 × 2), 755(b_{2g}, 0) cis-$AuH_2D_2^-$: 1906(407), 1906(407), 1303(478), 1303(477), ... trans-$AuH_2D_2^-$: 2030(0), 1724(1188), 1436(0), 1227(579), ... AuD_4^-: 1436(0), 1435(0), 1226(588 × 2), 566(0), 563(16), 542(15 × 2), 534(0)
$Au(H_2)^+$[b]	$^1A_1$	1.708 0.911	2596(a_1, 79), 1603(b_2, 23), 936(a_1, 86)
AuH_2^+[b]	$^1A_1$	1.541 76.7°	2292(a_1, 188), 2247(b_2, 85), 672(a_1, 8)

[a] The MH_2^- ions are 55, 62, and 65 kcal/mol more stable than the MH_2 molecules, respectively, Cu to Ag to Au. [b] $Au(H_2)^+$ is 184 kcal/mol higher than AuH_2, and AuH_2^+ is 7 kcal/mol higher than $Au(H_2)^+$.

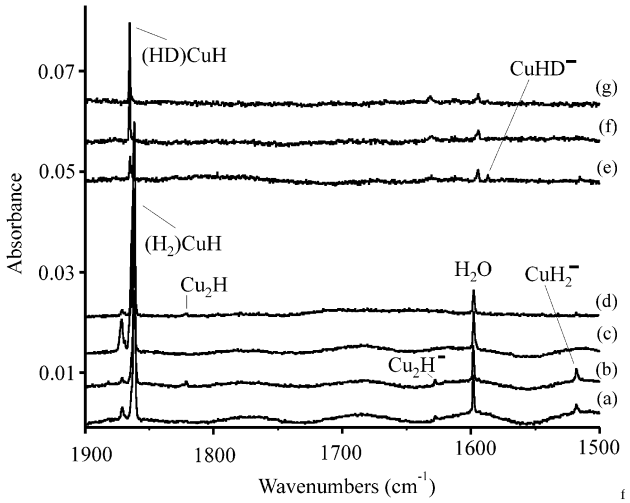

Figure 2. Infrared spectra of Cu co-deposited with pure normal H_2 or pure HD at 3.5 K for 25 min: (a) Cu + H_2, (b) after annealing to 6.0 K, (c) after λ > 240 nm photolysis, (d) after annealing to 6.5 K, (e) Au + HD, (f) after annealing to 7.3 K, (f) after λ > 240 nm photolysis, and (g) after annealing to 7.0 K.

H/D ratios and are near the very strong σ_u modes computed for linear AgH_2^- at 1444.7 cm^{-1} and AgD_2^- at 1031.3 cm^{-1}. The observed H/D ratios are again less than the calculated ratio 1.401 because of anharmonicity. Even though the ground state $^2B_2$ AgH_2 molecule is 30 kcal/mol above Ag + H_2, in agreement with previous calculations,[15] the AgH_2^- anion is 66 kcal/mol (B3LYP) more stable than AgH_2. Similar agreement is found for $AgHD^-$ in argon, where the calculated Ag−H and Ag−D frequencies at 1543.2 and 1076.9 cm^{-1} are 6.8 and 4.4% higher than the calculated σ_u modes of AgH_2^- and AgD_2^-, and the observed bands are 4.9 and 3.5% higher (Tables 1 and 2). These comparisons strongly support our identification of AgH_2^-. The linear PdH_2^- anion was observed slightly lower at 1247 cm^{-1} in similar argon matrix experiments.[42]

AuH_2^- and AuD_2^-. Laser-ablated gold experiments were repeated using as low laser energy as possible in order to trap charged species. Another pure deuterium experiment with gold is illustrated in Figure 4, where hydrogen spectra are also compared. The strong 1198.6 cm^{-1} $(D_2)AuD_3$ band is observed as before,[38] but weaker 1212.2 and 1182.3 cm^{-1} bands are enhanced using lower laser energy. Photolysis (λ > 530 nm) destroyed the weaker 1182.3 cm^{-1} peak and increased the 1212.2 cm^{-1} band, and irradiation at λ > 380 nm decreased the 1212.2 cm^{-1} feature, but λ > 290 nm photolysis regenerated the band at 1213.6 cm^{-1}. Final 8.0 K annealing destroyed all but the strongest 1198.6 cm^{-1} $(D_2)AuD_3$ absorption. Similar new gold experiments with hydrogen gave the strong 1661.5 cm^{-1} band of $(H_2)AuH_3$ and weaker, new 1676.4 and 1636.0 cm^{-1} absorptions. Annealing and photolysis (λ > 530 nm) destroyed the 1636.0 cm^{-1} peak and decreased the 1676.4 cm^{-1}

(42) Andrews, L.; Wang, X.; Alikhani, M. E.; Manceron, L. *J. Phys. Chem. A* **2001**, *105*, 3052 (Pd + H_2).

Table 3. States, Structures, and Vibrational Frequencies (cm^{-1}) Calculated for Copper, Silver, and Gold Hydrides Using B3LYP/6-311++G(d,p)/SDD

species	state	Å, deg	frequencies, cm^{-1} (symmetry, intensities, km/mol)
CuH	$^1\Sigma$	1.460	CuH: 1922(50); CuD: 1371(25)
CuH_2	$^2B_2$	1.511	CuH_2: 1792(a_1,9), 1645(b_2,17), 658(a_1,82)
		123.3°	
$Cu(H_2)^{+a}$	$^1A_1$	1.748	$Cu(H_2)^+$: 3793(a_1, 40), 1113(b_2, 24), 841(a_1, 20)
		0.788	
CuH_2^{-b}	$^1\Sigma_g^+$	1.562	CuH_2^-: 1666(σ_g, 0), 1492(σ_u, 919), 654(π_u, 242 × 2)
AgH	$^1\Sigma$	1.620	AgH: 1775(65); AgD: 1262(33)
AgH_2	$^2B_2$	1.662	1643(a_1,4), 1508(b_2,4), 522(a_1,84)
		119.1°	
AgH_2^{-b}	$^1\Sigma_g^+$	1.706	1594(σ_g, 0), 1428(σ_u, 987), 617(π_u, 217 × 2)
AuH	$^1\Sigma^+$	1.546	AuH: 2227(15); AuD: 1580(8)
AuH_2	$^2B_2$	1.619	AuH_2: 1995(a_1, 2), 1742(b_1, 1), 666(a_1, 33)
		128.6°	AuHD: 1889(2), 1305(1), 579(25)
			AuD_2: 1413(1), 1237(0.3), 473(17)
AuH_2^{-b}	$^1\Sigma_g^+$	1.670	AuH_2^-: 1939(0), 1629(1100), 736(61 × 2)
			$AuHD^-$: 1815(367), 1234(1457), 639(45 × 2)
			AuD_2^-: 1372(0), 1158(549), 523(29 × 2)
AuH_4^-	$^1A_{1g}$	1.649	AuH_4^-: 2052(0), 2050(0), 1726(1175 × 2), 814(0), 800(48), 786(0), 781(34 × 2)
			AuD_4^-: 1452(0), 1450(0), 1230(636 × 2), 576(0), 571(23), 556(0), 555(19 × 2)
$Au(H_2)^{+c}$	$^1A_1$	1.781	3103(a_2, 73), 1367(b_2, 24), 876(a_1, 61)
		0.847	
AuH_2^{+c}	$^1A_1$	1.540	2302(a_1, 186), 2253(b_2, 67), 621(a_1, 9)
		74.6°	

[a] $Cu(H_2)^+$ is 155 kcal/mol higher energy than CuH_2. [b] The MH_2^- ions are −57, −66, and −68 kcal/mol more stable than the MH_2 molecules, respectively, Cu to Ag to Au. [c] $Au(H_2)^+$ is 188 kcal/mol higher energy than AuH_2, and AuH_2^+ is 6 kcal/mol higher than $Au(H_2)^+$.

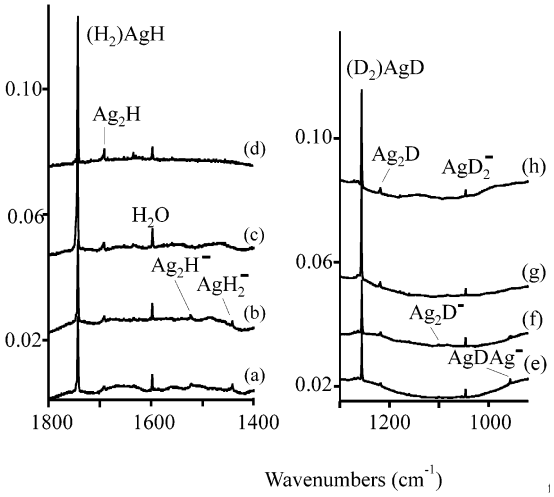

Figure 3. Infrared spectra of laser-ablated silver co-deposited with pure normal H_2 or pure normal D_2 at 3.5 K for 25 min: (a) Ag + H_2, (b) after annealing to 6.0 K, (c) after λ > 240 nm photolysis, (d) after annealing to 6.6 K, (e) Ag + D_2, (f) after annealing to 6.5 K, (g) λ > 240 nm photolysis, and (h) after annealing to 7.5 K.

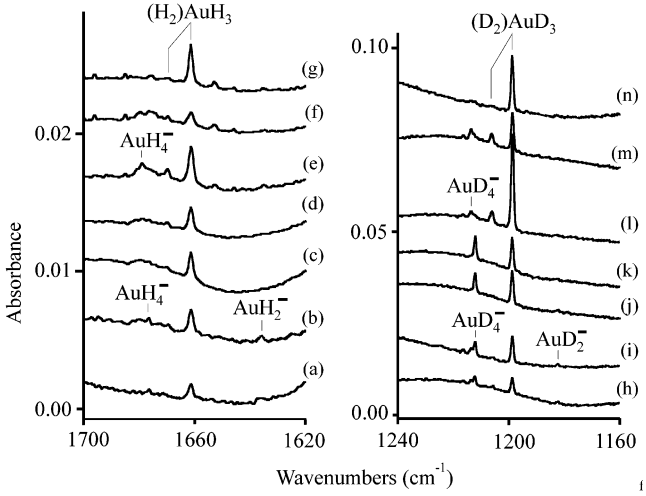

Figure 4. Infrared spectra of laser-ablated gold co-deposited with pure normal H_2 or pure normal D_2 at 3.5 K: (a) Au + H_2 deposited for 12 min, (b) Au + H_2 deposited for 12 min more, (c) after annealing to 5.3 K, (d) after λ > 530 nm photolysis, (e) after λ > 290 nm photolysis, (f) after λ > 240 nm photolysis, (g) after annealing to 6.0 K, (h) Au + D_2 deposited for 12 min, (i) Au + D_2 deposited for 12 min more, (j) after annealing to 7.0 K, (k) after λ > 530 nm photolysis, (l) after λ > 290 nm photolysis, (m) after λ > 240 nm photolysis, and (n) after annealing to 8.0 K.

band, but further photolysis (λ > 290 nm) increased the band at 1678.8 cm^{-1}. The photosensitive 1636.0 and 1182.3 cm^{-1} bands are isotopic counterparts (ratio 1.384). Finally, mixed isotopic experiments provide diagnostic information for the 1676.4 and 1212.2 cm^{-1} bands. Two experiments with pure H_2 + D_2 gave essentially the same positions for the new, stronger band, 1681.3 and 1211.3 cm^{-1}, but HD produced distinctly different 1840.4 and 1280.4 cm^{-1} absorptions that showed the same demise with λ > 380 nm photolysis as the 1676.4 and 1212.2 cm^{-1} bands, and exhibited sharp lower frequency site splittings at 1833.1, 1828.0 and 1275.3, 1272.4 cm^{-1}, which define similar band contours. We have no candidate absorptions for $HAuD^-$: it is likely that $HAuD^-$ quickly adds HD to form cis-$AuH_2D_2^-$ in solid HD.

Our BPW91 calculation using the relativistic SDD pseudopotential predicts a linear centrosymmetric AuH_2^- anion, analogous to $AuCl_2^-$,[4] with a very strong antisymmetric (σ_u) mode at 1641.6 cm^{-1} and AuD_2^- counterpart at 1167.1 cm^{-1}, and the B3LYP functional gives slightly lower 1629.3 and 1158.4 cm^{-1} frequencies, respectively. Our 1.668 and 1.670 Å bond lengths are slightly shorter than found previously (1.706 Å).[6] On the basis of the above excellent agreement, and like agreement between calculated and observed frequencies for isotopic CuH_2^- and AgH_2^- anions, which is summarized in Table 4, the 1636.0 cm^{-1} band is assigned to AuH_2^- in solid hydrogen and the 1182.3 cm^{-1} band to AuD_2^- in solid

Table 4. Comparison of Observed and Calculated Frequencies (cm^{-1}) for Coinage Metal Hydride Anions

	CuH_2^-	CuD_2^-	AgH_2^-	AgD_2^-	AuH_2^-	AuD_2^-	AuH_4^-	AuD_4^-
obs[a]	1517.8	1107.3	1442.4	1045.9	1636.0	1182.3	1676.4	1212.2
BPW91[b]	1501.0	1078.1	1444.7	1031.3	1641.6	1167.1	1724.4	1226.4
Δ[c,d]	(−1.1%)	(−2.6%)	(+0.2%)	(−1.4%)	(+0.3%)	(−1.3%)	(+2.9%)	(+1.2%)
BPW91[e]	1507.3	1082.6	1439.6	1027.4	1639.8	1165.8	1714.3	1219.2
Δ[c]	(−0.7%)	(−2.2%)	(−0.2%)	(−1.8%)	(+0.2%)	(−1.4%)	(+2.2%)	(+0.6%)
B3LYP[b]	1492.1	1071.7	1428.5	1019.8	1629.3	1158.4	1726.3	1227.9
Δ[c,d]	(−1.7%)	(−3.2%)	(−1.0%)	(−2.6%)	(−0.4%)	(−2.0%)	(+3.0%)	(+1.3%)

[a] Observed in solid H_2 or D_2 at 3.5 K. [b] Calculated with 6-311++G(d,p) and SDD. Unscaled frequencies given to 0.1 cm^{-1} in order to more accurately evaluate the mechanical effect of H/D substitution. [c] Calculated minus observed expressed as percent of observed frequency. [d] The LANL2DZ pseudopotential and basis work poorly for these dihydride anions using both density functionals. The strong σ_u frequencies are predicted 7.6 and 7.3% too low for AuH_2^- (BPW91 and B3LYP), respectively, and 9.1 and 8.8% too low for AuD_2^-. The σ_u frequencies are 8.7 and 8.9% too low (BPW91 and B3LYP, respectively) for AgH_2^-, 10.1 and 11.0% too low for AgD_2^-, 10.8 and 10.4% too low for CuH_2^-, and 12.2 and 12.4% too low for CuD_2^-. Likewise BPW91/LANL2DZ predicts the e_u frequency 5.0 and 6.6% too low for AuH_4^- and AuD_4^- (BPW91). [e] Calculated with larger 6-311++G(3df,3pd) basis set for H and SDD for metal.

deuterium. The AuH_2^- frequency is calculated within 0.4% and the AuD_2^- frequency within 2% because we are comparing calculated harmonic and observed anharmonic frequencies. The observed H/D ratio 1.384 is again less than the calculated ratio 1.407 owing to anharmonicity. We note that the LANL2DZ pseudopontial does not predict frequencies nearly as accurately for these dihydride anions (Table 4), although it works well for neutral species.[36] Neon experiments with 5% H_2 produced a new absorption at 1638.6 cm^{-1} that decreased on annealing to 7 K and disappeared on $\lambda > 380$ nm photolysis, which is assigned to AuH_2^- in solid neon. The $Au(I)H_2^-$ anion is very photosensitive in solid hydrogen in part because Au(III) compounds are stable for gold.

AuH_4^- and AuD_4^-. The 1212.2 cm^{-1} band with Au in pure D_2 was observed previously,[38] but it was assumed to be a satellite of $(D_2)AuD_3$. This 1212.2 cm^{-1} band decreased on 8.0 K annealing, which had little effect on the $(D_2)AuD$ and $(D_2)AuD_3$ absorptions, but it was regenerated at 1213.6 cm^{-1} by $\lambda > 290$ and 240 nm photolysis.[38] New experiments using lower laser energy increased the 1212.2 cm^{-1} band relative to $(D_2)AuD$ and $(D_2)AuD_3$ absorptions. After 7.0 K annealing (Figure 4) the 1212.2 cm^{-1} band is over half of the 1198.6 cm^{-1} band, but $\lambda > 290$ nm irradiation decreases the 1212.2 cm^{-1} band and increases bands at 1213.6 and 1205.9 cm^{-1} and the $(D_2)AuD$ and $(D_2)AuD_3$ absorptions, whereas $\lambda > 220$ nm photolysis further increases the 1213.6 cm^{-1} band but decreases $(D_2)AuD_3$ and markedly increases $(D_2)AuD$. The 1205.9 cm^{-1} absorption is a photochemical site of the 1198.6 cm^{-1} $(D_2)AuD_3$ absorption.

Additional Au experiments with pure H_2 employed even lower laser energy, and the spectrum in Figure 4 also shows a new 1676.4 cm^{-1} absorption above the 1661.5 cm^{-1} band of $(H_2)AuH_3$. The new 1676.4 cm^{-1} band is extremely photosensitive: it decreases by half relative to the 1661.5 cm^{-1} absorption *during recording the spectrum*. The 1676.4 cm^{-1} band is destroyed by visible photolysis, but regenerated at 1678.8 cm^{-1} by $\lambda > 290$ nm irradiation: it is also destroyed by annealing and again regenerated by $\lambda > 290$ nm photolysis. Hence, the 1676.4 and 1212.2 cm^{-1} bands are counterparts in sensitive behavior and regeneration, and they exhibit the 1.383 H/D ratio that is typical of gold hydride vibrations (1661.5/1198.6 = 1.386 for $(H_2)AuH_3$ and 2164.0/1556.5 = 1.390 for $(H_2)AuH$).

Pure H_2 and pure D_2 favor the 1676.4 and 1212.2 cm^{-1} bands (ratio 1.383), which are assigned to AuH_4^- and AuD_4^-. The photogenerated counterparts at 1678.8 and 1213.6 cm^{-1} (ratio 1.383) are also due to AuH_4^- and AuD_4^- produced by a different route. We point out here that similar thermal gold experiments in solid H_2 with narrow band 265 nm photolysis produced $(H_2)AuH$ and AuH_2 without the absorptions assigned here to AuH_2^- and AuH_4^-.[26]

Our BPW91 calculation using SDD for gold predicts very strong 1724.4 and 1226.4 cm^{-1} antisymmetric stretching (e_u) modes for the square-planar AuH_4^- and AuD_4^- species, which is isostructural to $AuCl_4^-$.[43,44] These calculated frequencies are 1−3% higher than the observed absorptions. The B3LYP functional (Table 3) gives slightly higher frequencies. The observed (1.383) and calculated (1.406) H/D ratios are nearly the same for AuH_4^- and AuH_2^-, as both of these vibrational modes involve linear H−Au−H linkages. Our DFT bond length (1.653 Å) is almost the same (1.652 Å) as computed previously for AuH_4^-, and these earlier workers predicted AuH_4^- to be a stable anion.[7] However, the confirmation for this assignment comes from $H_2 + D_2$ and HD isotopic substitution (Figure 5). Unlike the case for a tetrahedral product, such as the group 3 and 13 MH_4^- anions,[45,46] where the same $MH_2D_2^-$ species are produced from $H_2 + D_2$ and 2 HD, the square-planar anion has cis and trans dideuterio isomers. Our calculations show that the observable trans isomer

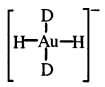

frequencies (antisymmetric vibrations of linear subunits) are unchanged from AuH_4^- and AuD_4^-, but the cis isomer

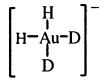

gives a substantially different spectrum with strong bands 10.6% and 6.3% higher than the pure isotopic species. Our $H_2 + D_2$ spectrum finds new 1681.3 and 1211.3 cm^{-1} bands essentially unchanged from pure H_2 and pure D_2 values (considering that pure $H_2 + D_2$ is a different host). Furthermore, pure HD gives two new bands at 1840.4 and 1280.4 cm^{-1}, which are 9.8 and 5.6% higher than the bands observed for AuH_4^- and AuD_4^-. This we consider to be exceptional agreement between the calculated and observed isotopic frequencies, and we offer this combined experimental and theoretical confirmation for our preparation of isolated AuH_4^- in solid hydrogen. We also note that annealing the H_2/D_2 sample to 7.5 K removes the 1681

(43) Melnick, M.; Parish, R. V. *Coord. Chem. Rev.* **1986**, *70*, 157.
(44) Degen, I. A.; Rowlands, A. J. *Spectrochim. Acta* **1991**, *47A*, 1263.

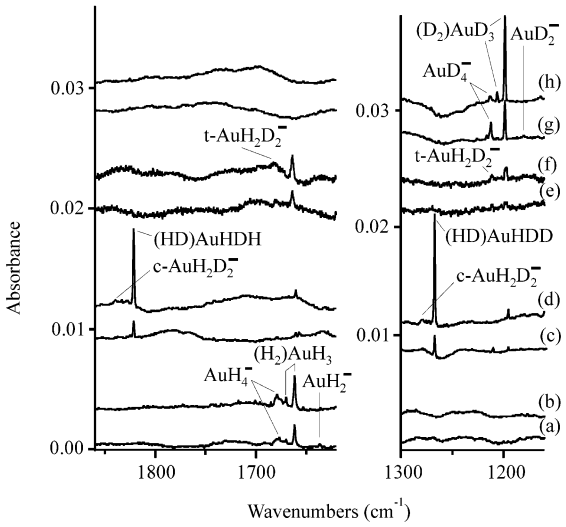

Figure 5. Infrared spectra in the 1860−1620 and 1300−1160 cm^{-1} regions for laser-ablated Au co-deposited with pure hydrogen isotopic samples at 3.5 K for 14−24 min: (a) Au + H_2, (b) after $\lambda > 290$ nm photolysis, (c) Au + HD, (d) after $\lambda > 290$ nm photolysis, (e) Au + 50% H_2 + 50% D_2, (f) after $\lambda > 290$ nm photolysis, (g) Au + D_2, and (h) after $\lambda > 290$ nm photolysis.

and 1211 cm^{-1} absorptions for $AuH_2D_2^-$ but leaves the 1663 and 1198 cm^{-1} bands for (L)AuH_3 and (L)AuD_3 unchanged. Charged species are clearly more vulnerable on annealing, as charge neutralization can occur.

Atomic gold cations are also formed in the ablation process along with electrons, and in experiments with CO, the AuCO carbonyl and small amounts of $AuCO^+$ and $AuCO^-$ were observed.[27,28] What then is the fate of Au^+ in solid hydrogen? Surely $Au(H_2)^+$ is made, but it is likely to be further coordinated to $Au(H_2)_n^+$, and broad absorption would make its detection very difficult.

Chemical Comparisons. It is interesting to compare the group 11 dihydride anions with the isoelectronic group 12 dihydrides, which have been observed by matrix isolation spectroscopy. Calculated structures for the coinage metal dihydride anions are illustrated in Figure 6. The strong antisymmetric H−M−H stretching fundamentals are 1870, 1753, and 1896 cm^{-1} for ZnH_2, CdH_2, and HgH_2, respectively, in solid argon,[39,47] which are considerably higher than these modes for the MH_2^- anions at 1518, 1442, and 1636 cm^{-1} in solid hydrogen. Note the same periodic relationship in the group 11 and 12 dihydride frequencies, which has been explained by relativistic effects for gold and mercury.[48] The present observation of stable AuH_2^- and AuH_4^- anions can be attributed in part to relativistic effects.[6,7] Finally, our AuH_4^- anion isolated in solid hydrogen with e_u mode at 1676 cm^{-1} can be compared with recent computations for the square-planar isoelectronic HgH_4 molecule,[49] which predict the strong mode at 1959 cm^{-1}, and with the known square-planar PtH_4^{2-} dianion with sodium cations in the solid compound,[50] which has a comparable 1.639 Å bond length.

AuH_2 Molecule. Of the group 11 dihydride molecules, we believe that AuH_2 has the best chance to survive in the matrix.

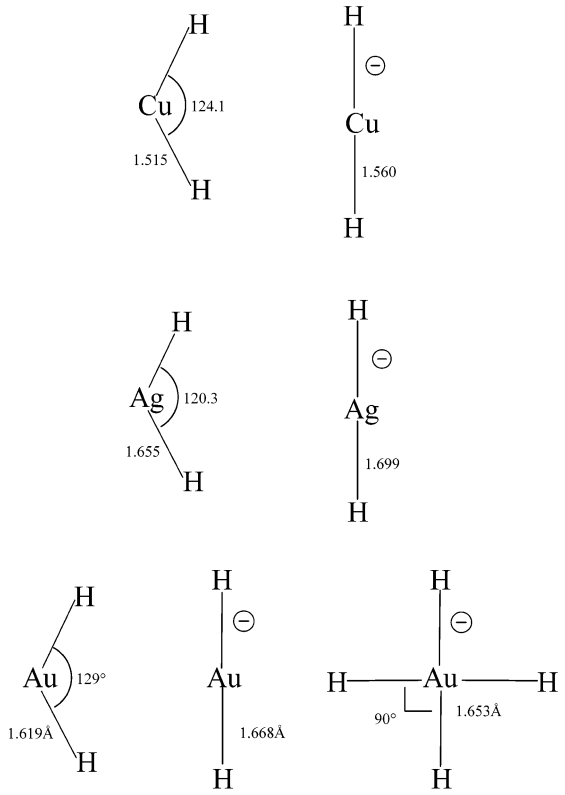

Figure 6. Structures calculated (with BPW91/6-311++G(d,p)/SDD) for CuH_2, CuH_2^-, AgH_2, AgH_2^-, AuH_2, AuH_2^-, and AuH_4^-.

This hypothesis is based largely on the greater strength of the Au−H bond: experimental dissociation energies for CuH, AgH, and AuH are 63, 53, and 74 kcal/mol, respectively.[24] Weak, new bands are observed at 638.1 and 457.0 cm^{-1} for laser-ablated Au in solid H_2 and in solid D_2 (Figure 7).[51] These bands decrease on visible photolysis but increase on the 240 nm photolysis needed to activate gold for reaction with H_2 and increase on annealing following 240 nm photolysis. With pure HD a stronger band at 570.6 cm^{-1} increases slightly on annealing to 6.5 K, changes little on visible and 290 nm photolysis, but doubles on 240 nm irradiation and remains on annealing to 7.4 K (Figure 7). These bands are assigned to AuH_2, AuHD, and AuD_2. In like fashion our pure H_2 + D_2 experiment gave a weak 638 cm^{-1} band, but the 450 cm^{-1} region was too poor in signal to observe the lower absorption. A weak 560.2 cm^{-1} band appears on 240 nm photolysis, which is probably due to (D_2)AuH: the (H_2)AuH molecule exhibits similar behavior. Complementary thermal gold/pure normal hydrogen (deuterium) experiments with 265 nm photolysis into the gold $^2P_{1/2}$ state produce the same 638.1 and 457.0 cm^{-1} absorptions, as well as (H_2)AuH and (D_2)AuD, in solid hydrogen and deuterium, respectively.[26]

The best MRSDCI calculations[15] find a $^2B_2$ ground state AuH_2 molecule (1.62 Å, 127°) 20 kcal/mol above Au + H_2, and for AuH_2 to be trapped in the hydrogen matrix, an energy barrier must separate it from the lower energy Au + H_2 products. We calculate the two H atoms in AuH_2 to be 2.92 Å apart (BPW91),

(45) Pullumbi, P.; Bouteiller, Y.; Manceron, L. *J. Chem. Phys.* **1994**, *101*, 3610.
(46) Wang, X.; Andrews, L. *J. Am. Chem. Soc.* **2002**, *124*, 7610.
(47) Legay-Sommaire, N.; Legay, F. *Chem. Phys. Lett.* **1993**, *207*, 123.
(48) Pyykkö, P. *Chem. Rev.* **1988**, *88*, 563.
(49) Pyykkö, P.; Straka, M. *J. Chem. Soc., Chem. Commun.* **2002**, 1720.
(50) Bronger, W. *Angew. Chem., Int. Ed. Engl.* **1991**, *30*, 759.

(51) The 457.0 cm^{-1} band was first assigned to the D−Au−D bending mode of the $(D_2)AuD_3$ complex.[37,38] More solid D_2 experiments show that the weaker 457.0 cm^{-1} band does not track with the 1198.6 cm^{-1} absorption. In thermal gold experiments[26] the 457.0 cm^{-1} band is strong and the 1198.6 cm^{-1} band is absent.

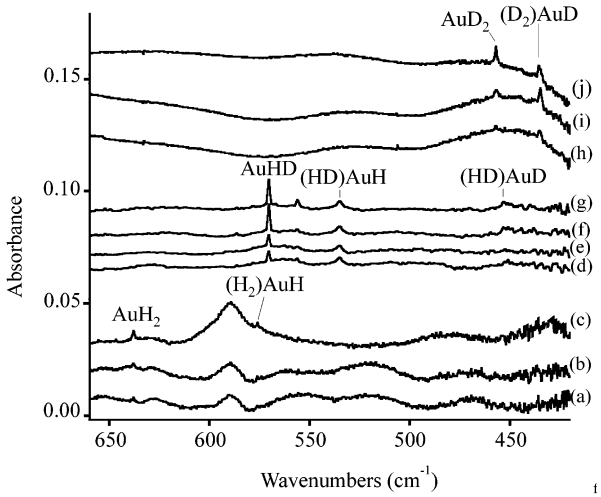

Figure 7. Infrared spectra in the 660−420 cm^{-1} region for laser-ablated Au co-deposited with pure hydrogen isotopic samples at 3.5 K for 25 min: (a) Au + H_2, (b) after $\lambda > 240$ nm photolysis, (c) after annealing to 6.4 K, (d) Au + HD, (e) after $\lambda > 290$ nm photolysis, (f) after $\lambda > 240$ nm photolysis, (g) after annealing to 7.5 K, (h) Au + D_2, (i) after $\lambda > 240$ nm photolysis, and (j) after annealing to 9.0 K.

and the H−Au−H angle must be highly activated close to the 27° value required for the H−H distance (0.75 Å) of diatomic H_2. Accordingly, the CASSCF bending potential surface for the $^2B_2$ state AuH_2 molecule rises about 20 kcal/mol at a 60° angle, where crossing to the $^2A_1$ surface leads to dissociation to Au (^2S) + H_2.[15a] Hence, a barrier to dissociation is calculated for AuH_2.

Our BPW91 calculations (Tables 2 and 3) predict almost the same structure for AuH_2 and very weak stretching modes, but a much more intense bending mode at 666 cm^{-1}. This bending mode is calculated at 579 cm^{-1} for AuHD and at 473 cm^{-1} for AuD_2. The 638.1, 570.6, and 457.0 cm^{-1} bands are in excellent agreement with the calculated bending frequencies for isotopic AuH_2 molecules, which strongly supports this AuH_2 assignment.[52]

Mechanisms. The straightforward reaction mechanism includes the formation of MH molecules in endothermic reaction 1 driven by the excess electronic/kinetic energy[25] in the laser-ablated metal atoms. Electrons produced in the ablation process[27,28] are subsequently captured by hydrogen to form hydride anions for exothermic reaction with the MH molecules to make the stable linear $M(I)H_2^-$ anions, reactions 2 and 3. In contrast thermal Au atoms in pure deuterium gave no metal deuteride products,[53] but 265 nm resonance photolysis produced $(D_2)AuD$ and AuD_2 with no anions.[26] Our computed electron detachment energies for CuH_2^- and AuH_2^-, 55 and 65 kcal/mol, respectively, are much less than the experimental values for the more stable chloride complexes $CuCl_2^-$ and $AuCl_2^-$, 100 and 109 kcal/mol.[2,4] Reactions 1, 2, and 3 explain the argon matrix reactions, as CuH_2^-, $HCuD^-$, and CuD_2^- were all observed using both HD and H_2 + D_2 mixtures. However, in pure HD only $HCuD^-$ and no CuH_2^- and CuD_2^- were observed. Hence, the mechanism in the pure hydrogen host involves the complete reagent molecule, which implies that the MH_2 molecule remains intact long enough to capture an electron from the ablation process, reaction 4. Even though earlier workers have questioned the stability of CuH_2,[14,21] a small yield of CuH_2 appears to survive in the hydrogen matrix.[26] This means that MH_2 formed in reaction 5 from ^2P excited metal atoms [^2P is above ^2S by 87.3, 84.5, and 106.8 kcal/mol, for Cu, Ag, Au, respectively][54] has a sufficiently long lifetime to capture an electron before decomposition, and the anion product of reaction 4 is trapped in the solid hydrogen matrix. The relative energies of Au + H_2 species are summarized in Figure 8: we use the best available energies including experimental values,[24,53] the MRSDCI energy[15] for AuH_2, and our B3LYP energy for AuH_2^-. This diagram illustrates how excited Au(^2P) initiates the reactions that lead to the observed products.

$$M\,(^2S) + H_2\,(^1\Sigma_g^+) \rightarrow MH\,(^1\Sigma^+) + H\,(^2S) \quad [\Delta E = 40, 51, 29\ \text{kcal/mol}]^{24} \quad (1)$$

$$H\,(^2S) + e^- \rightarrow H^-\,(^1S) \quad [\Delta E = -17\ \text{kcal/mol}]^{55} \quad (2)$$

$$MH\,(^1\Sigma^+) + H^-(^1S) \rightarrow MH_2^-\,(^1\Sigma_g^+) \quad [\Delta E = -67, -68, -77\ \text{kcal/mol}]^{56} \quad (3)$$

$$MH_2\,(^2B_2) + e^- \rightarrow HMH^-\,(^1\Sigma_g^+) \quad [\Delta E = -57, -66, -68\ \text{kcal/mol}]\ \text{(B3LYP)} \quad (4)$$

$$[\Delta E = -55, -62, -65\ \text{kcal/mol}]\ \text{(BPW91)}$$

$$M^*\,(^2P) + H_2\,(^1\Sigma_g^+) \rightarrow MH_2^* \quad (5)$$

Another interesting reaction, reaction 6, to make square-planar $M(III)H_4^-$ anions, is too endothermic for the Cu and Ag matrix reactions; however, the greater stability of Au(III) is revealed by the reaction energetics. The solid hydrogen and deuterium environments apparently help to form the AuH_4^- and AuD_4^- anions, and reaction 3 activates reaction 6 for gold.

$$MH_2^- + H_2 \rightarrow MH_4^-\,(^1A_{1g}) \quad [\Delta E = 22, 30, 13\ \text{kcal/mol}]\ \text{(B3LYP)} \quad (6)$$

$$[\Delta E = 16, 23, 9\ \text{kcal/mol}]\ \text{(BPW91)}$$

The mixed isotopic experiments also provide mechanistic information. The HD reaction gives predominantly the cis

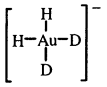

product, and the H_2 + D_2 reaction gives only trans products including

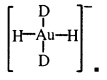

This means that some of the AuH_2^* product of reaction 5 electron captures and H_2 captures (reaction 6) before relaxation and decomposition of the AuH_2 molecule to AuH + H in the hydrogen matrix. Hence, the energy needed to drive reaction 6 is provided in the original excitation process required for

(52) The present AuH_2 molecule cannot be compared with defect "complexes" containing Au and H in silicon where H is bonded to Si adjacent to Au; see: Evans, M. J.; Stavola, M.; Weinstein, M. G.; Uftring, S. J. *Mater. Sci. Eng.* **1999**, *B58*, 118.

(53) Gruen, D. M.; Bates, J. K. *Inorg. Chem.* **1977**, *16*, 2450.

(54) Moore, C. E. *Atomic Energy Levels, Vol. II*; National Bureau of Standards, U.S., 1952.

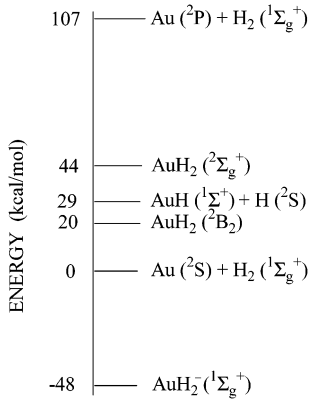

Figure 8. Relative energies of Au + H_2 reagents and products.

reaction 5, which is a 263 nm absorption to form Au (^{2}P) in solid deuterium.[51] Once trapped in the solid hydrogen matrix at 3.5 K, there must be an energy barrier to decomposition of AuH_4^- by the reverse of reaction 6: one 90° angle in AuH_4^- must close enough to reduce the H−H distance from 1.653 Å $\times \sqrt{2}$ to the diatomic 0.75 Å bond length.

The matrix photochemistry of the CuH_2^-, AgH_2^-, AuH_2^-, and AuH_4^- anions is of interest, as the anions may eventually be characterized in the gas phase by PES. However, the matrix photochemistry is complicated by photodetachment from other anions such as H^- and M^- (the electron affinities of Cu, Ag, and Au are 28, 30, and 53 kcal/mol, respectively)[57] and subsequent reattachment. The higher UV photon energy required to destroy CuH_2^- and AgH_2^- in solid hydrogen, relative to the 530 nm photodestruction of AuH_2^-, is probably due to reaction 6 for gold and the lack of reaction 6 for silver and copper.

The coinage metal atoms have significant electron affinities, and a possible role for M^- anions and these experiments must be considered. Ground state M^- anions are isoelectronic with Zn, Cd, and Hg and unreactive with H_2. However, the ^{3}P states are reactive,[39,47] and near-ultraviolet excitation[58] is expected to lead to reaction 8. In fact the growth of AuH_4^- on 290 nm photolysis, when Au (^{2}P) excitation to form (H_2)AuH requires $\lambda > 220$ nm (actually 265 nm) photolysis, is probably due to this reaction.

$$M\,(^2S) + e^- \rightarrow M^-\,(^1S) \qquad [\Delta E = -28, -30, -53\ \text{kcal/mol}][57] \quad (7)$$

$$M^-\,(^1S) + H_2 \xrightarrow{UV} M^-\,(^3P) + H_2 \rightarrow MH_2^-\,(^1\Sigma_g^+) \quad (8)$$

$$Au^-\,(^1S) + 2H_2 \xrightarrow{290\ nm} Au^-\,(^3P) + 2H_2 \rightarrow AuH_4^-\,(^1A_{1g}) \quad (9)$$

We suggest that the 1676.4 and 1212.2 cm^{-1} matrix sites for AuH_4^- and AuD_4^- result from reactions 3 and 6 in sequence and that the 1678.8 and 1213.6 cm^{-1} matrix sites produced on 290 nm photolysis are due to the Au^- reaction 9. Complementary thermal gold experiments with 265 nm resonance photolysis produced (H_2)AuH and AuH_2 but no gold hydride anions.[26]

Our identification of AuH_2 in solid hydrogen suggests that the products of reaction 1 must back react on annealing to give some AuH_2, exothermic reaction 10. In the case of CuH and AgH the analogous back H atom reaction instead gave Cu, Ag, and H_2 in solid krypton.[21] However, Au presents a larger cross-section for the H atom reaction, and the resulting AuH bond is stronger; hence, we believe that reaction 10 is likely to form AuH_2 in pure hydrogen on annealing to 6.5 K, as is observed. However, no isotopic scrambling is observed in our HD experiment, Figure 7 (d, e, f), so most of the product of reaction 11 must be stabilized by the matrix. Complementary thermal gold experiments[26] employed precise 265 nm excitation of the $^2P_{1/2}$ gold state (using a dielectric notch filter) for activating reaction 12.

$$H\,(^2S) + AuH\,(^1\Sigma^+) \rightarrow AuH_2\,(^2B_2) \quad [\Delta E = -28\ \text{kcal/mol}] \quad (10)$$

$$Au\,(^2P) + HD \rightarrow AuHD \quad (11)$$

$$Au\,(^2P) + H_2 \rightarrow AuH_2\,(^2B_2) \quad (12)$$

Another interesting difference is noted in the gold reactions in pure H_2, pure HD, and pure D_2.[59] Both normal H_2 and normal D_2 samples employed here are ortho and para nuclear spin isomer mixtures.[60] This means that some molecules in the solids are still in $J = 1$ rotational states and suggests that relaxation of the AuH_2* product of reaction 5 will be slower as a result of residual rotational energy in the condensing hydrogen gas. However, HD with different nuclei can relax to the $J = 0$ rotational state and should likewise relax and trap AuHD more efficiently on cooling to 3.5 K. Hence, the higher yield of AuHD and the lack of isotopic scrambling in the HD experiment can be rationalized.

Hydrogen Storage Applications. We believe that the basic science reported here can be used to develop efficient new hydrogen storage materials. The stable group 11 dihydride anions are unique in that the neutral metal dihydride molecule is unstable with respect to metal and dihydrogen. If copper dihydride anions can be synthesized in the solid state, possibly through hydrogen overpressure saturation of a sodium−copper alloy, or the reaction of NaH with spongy copper under excess hydrogen, electrical or thermal decomposition to release hydrogen gas should be possible at relatively low temperatures.[8,11]

Conclusions

In addition to the diatomic MH molecules and their dihydrogen complexes (H_2)MH, reactions of laser-ablated coinage metal atoms and electrons with H_2 in excess argon, neon, and pure hydrogen give the stable MH_2^- and AuH_4^- anions. These products are trapped in the condensing solids at 3.5 K and identified from matrix infrared spectra using isotopic substitution (HD, D_2, and $H_2 + D_2$) and comparison to isotopic frequencies computed by DFT. The stable linear MH_2^- anions are unique

(55) Berry, R. S. *Chem. Rev.* **1969**, *69*, 533.
(56) Reaction energetics computed at the B3LYP/6-311++G(d, p)/SDD level of theory for Cu, Ag, and Au, respectively. The BPW91 values are within 1 kcal/mol.
(57) Hotop, H.; Lineberger, W. C. *J. Phys. Chem. Ref. Data* **1985**, *14*, 731.
(58) B3LYP calculations predict Au^- (^{1}S) 51.0 kcal/mol below Au (^{2}S) (53.3 kcal/mol experimental) and Au^- (^{3}P) 67.6 kcal/mol higher; hence this excitation with near UV photolysis is straightforward.
(59) The solid H_2, D_2, and HD environments are also different. The H_2O bending mode is measured at 1598.2 cm^{-1} in normal solid H_2, at 1597.4 cm^{-1} in normal solid D_2, at 1597.8 cm^{-1} in a 50/50 mixture, and at 1594.6 cm^{-1} in solid HD. The full-widths at half-maximum are 1.0, 1.6, 1.4, and 1.8 cm^{-1}, respectively, suggesting the weakest interaction with H_2.
(60) Silvera, I. F. *Rev. Mod. Phys.* **1980**, *52*, 393.

in that their corresponding neutral molecules are higher energy and thus unstable to decomposition into $M + H_2$. However, the AuH_2 molecule is observed in laser-ablation and thermal gold-resonance photolysis experiments[26] and is the most stable of the group 11 dihydride molecules.

Further reaction of linear $HAuH^-$ with another H_2 molecule gives the square-planar AuH_4^- anion, which is identified from the different spectra for cis- and trans-$AuH_2D_2^-$ anions. The observation of an MH_4^- anion only for gold attests the stability of the higher Au(III) oxidation state and the effect of relativity on third-row transition metal bonding.[7,35,48]

It is impressive how well DFT using relativistic SDD effective core potentials works to predict experimental frequencies for the CuH_2^-, AgH_2^-, and AuH_2^- anions, particularly in view of the lack of anharmonic correction in the calculated frequencies. The BPW91 functional computes the strong σ_u frequencies approximately 1−2% too low with slightly larger percent deviations using B3LYP. For AuH_4^- and AuD_4^-, the BPW91 functional predicts the e_u modes 2.9 and 1.2% too high, and the B3LYP functional comes in at 3.0 and 1.3% too high.

Acknowledgment. We thank the NSF (Grant CHE00-78836) for financial support.

JA036307Q